J. Phys. D: Appl. Phys. 26 (1993) 371–378. Printed in the UK

Luminescence spectra of germanosilicate optical fibres. I: radioluminescence and cathodoluminescence

M R Khanlary†, P D Townsend† and J E Townsend‡

† School of Mathematical and Physical Sciences, University of Sussex, Brighton BN1 9QH, UK
‡ ORC, University of Southampton, Southampton SO9 5NH, UK

Received 12 June 1992, in final form 10 November 1992

Abstract. Data are reported on the luminescence spectra generated by x-ray and electron irradiation of optical fibres, fibre preforms and silica. The impurities and imperfections in the fibre core have a higher luminescence efficiency than those in the substrate material. The core luminescence provides a major fraction of the total light emission, despite the fact that the core is a small fraction of the total fibre volume. A wide variety of overlapping emission bands are reported. The spectra are strongly temperature dependent but the component emission bands can generally be linked to either Ge impurities, giving the 400 nm band, exciton emission near 460 nm or other blue/uv bands linked to E′-type defects. Overall, the study of the fibre luminescence provides a sensitive technique for analysis of changes and repeatability of fibre fabrication.

1. Introduction

Luminescence measurements are among the most sensitive techniques for studying defects and trace impurities in insulators. There is a particularly large amount of literature on the imperfections in crystalline quartz and amorphous silica variations of SiO_2 but, not surprisingly, the luminescence results from different laboratories differ in detail, since the emission behaviour is highly sensitive to trace impurities. Nevertheless, there is general agreement that closely related point defects exist in both crystalline and glass SiO_2. The best characterized defects all involve broken oxygen bonds which act not only as electron traps but also as sites for forming complexes with impurities, new intrinsic linkages or structural relaxations. In terms of luminescence in the 200 to 800 nm region one expects signals from intrinsic relaxations of self-trapped excitons (STE), typically mentioned near 460 nm (2.7 eV), plus a variety of similarly positioned emission bands in which electron–hole recombination occurs at defect sites which are only slightly perturbed relative to the perfect silica tetrahedra. Such defect sites include the E′-type defects, peroxy bonds and their complexes. Additionally there are of course distinctly different emission bands where the transitions are localized at specific impurities, or as transitions within the energy levels of rare earth ions. Overall there are consistent reports of emission near 500 nm (2.5 eV), probably from extrinsic defect sites and 440 nm (2.8 eV) light assumed to be from relaxations of STE (Alonso *et al* 1983, Grinfelds *et al* 1984, Itoh *et al* 1988, 1989, 1990, Tanimura and Halliburton 1983, 1986, Trukhin and Plaudis 1979). In many examples the emission envelope peaks near 460 nm, for example in ion beam excitation where a wide range of defects and perturbed sites are stimulated together with transient defect structures (e.g. Abu Hassan and Townsend 1988, Wang *et al* 1991). Absolute values often differ slightly both from sample variations and from inconsistencies in correction of the recorded spectra. Higher energy emission from silica is seen at 295 and 234 nm (4.2 and 5.3 eV). Ion beam excited luminescence includes small bands near 280 and 640 nm (4.45 and 1.94 eV) (Jaque and Townsend 1981). However, orange emission is only seen in some samples and is quenched by ion beam radiation damage.

Defect models of quartz luminescence have been discussed, partly because quartz is used extensively in archaeological dating. Impurity induced distortions of the emitting sites are reviewed by McKeever (1984, 1985) and Yang and McKeever (1988, 1990a, b) in which they suggest important impurities are Ge, $[H_3O_4]^0$ and $[AlO_4]^0$—the Ge being an electron trap, whereas the others are hole traps. Recombination at the hole

0022-3727/93/030371+08$07.50

impurity sites shifts the wavelength of the emission of e–h recombination in quartz to 380 nm for the H_3O_4 and 470 nm for the AlO_4. There is strong evidence for such intrinsic impurity complexes as the relative sensitivity and emission wavelength of the luminescence are altered by both radiation and heat treatment of the samples.

The smaller amount of literature involving silica-based optical fibres is more difficult to interpret because, in addition to the waveguiding core which includes dopants such as germanium, phosphorus and chlorine to form a raised refractive index, the samples include a boundary layer (the cladding) and the structural silica-based glass on which the fibres are deposited. This latter feature is termed the substrate. Although it is optically of minor importance for the waveguide, it nevertheless forms more than 90% of the optical fibre structure and it is not as carefully prepared as the core. For luminescence studies where the energy is provided from the side of the fibre, for example with x-rays or UV light, the substrate can contribute significantly to the total luminescence. By contrast, cathodoluminescence, with electrons of say 10 keV, the electrons do not penetrate through the substrate into the core and one must use end-on excitation by directing the electron beam into a cross section of the fibre fragments so as to include the core luminescence.

At first sight it might be assumed that, because of the greater volume of substrate compared with the core, the luminescence signals from optical fibres will be dominated by the substrate. However, this is not the case and in most of the data reported here the luminescence efficiency of the core far exceeds that of the substrate, hence similar substrates with differently prepared cores show recognizably different signals. This is encouraging as it suggests that one can use luminescence techniques to probe some of the defect sites that exist in the optical fibres and even separate features which result from impurities and those which develop during fibre production and drawing. Ideally one might link the presence, or absence, of specific defects to the propagation losses or lasing performance of optical fibre devices. Where this is possible the defect data may then be fed back to the production stage to improve the quality of the fibre structures. This is technologically interesting even if one cannot specify unequivocal defect models for the various emission bands.

Luminescence can either be directly stimulated and recorded as during x-ray, electron or photon irradiation, or result from charge redistribution as electrons or holes are thermally liberated from metastable sites (i.e. thermoluminescence). The directly excited signals reveal information on a wider range of defect sites as they can respond to short-lived states, transitions between excited states, or involve transitions after band to band excitation. Such directly stimulated luminescence data are reported in this paper. Data relating to thermoluminescence are discussed separately in the following paper (part II). The two types of experiment are expected to complement one another.

2. Experimental procedure

Various samples of pure silica, fibre preforms, drawn optical fibres and, in some cases, powdered fibre material have been examined. No data for powdered samples are shown here but in practice the results quite closely resemble those obtained from fibre fragments made prior to grinding. This suggests that the luminescence spectra are not seriously perturbed by light being guided in the fibre and thus directed away from the luminescence spectrometer. In the fibre examples the plastic cladding was chemically removed. In order to make comparisons between the doped fibre material and nominally pure silica additional measurements were made with 'pure' silica in the form of Spectrosil B from Thermal Syndicate Ltd. This bulk silica has a total impurity content quoted as being below 0.2 ppm. All fibres and preforms were prepared at Southampton University, using previously described methods (Nagel *et al* 1982, Townsend *et al* 1987). Table 1 lists the various preforms and fibres, together with growth conditions and the dopants added in the core and cladding regions, which were used in this study. There are various stages which introduce defect structures. These include the initial deposition of a porous frit (i.e. the precursor of the core and cladding); for fibre lasers there is a further stage for chemical addition of laser dopants followed by a drying process. There is then a thermally activated collapse of the frit and substrate tube into a preform, and finally fibre drawing. Defect production can develop by thermodynamic processes, impurity clustering and retention of frit characteristics but it is assumed that the final heating stage of fibre pulling is likely to be most critical as many defects will anneal during the final heating phase. The melt temperature and drawing speed are therefore quoted. The list includes samples numbered ND297, ND324, ND326, ND414, ND416 and ND424. (Note that only a selection of the data is discussed in this paper.) All the preform samples have the same substrate material but differ in the additives in the core and cladding. Cladding regions frequently contain P and F ions. Any obvious effects from these impurities might be apparent in comparisons of fibres ND414 and ND416. Fibre number ND414 has P and F ions in the cladding, both at the 1% level, and Ge, Er and Yb in the core, whereas fibre type ND416 has a pure silica cladding interface region but Ge and Nd in the core. Both ND414 and ND416 have a minimal amount of Cl added. One might expect that the P and/or F impurities at such high concentrations would produce identifiable features in the luminescence. However, as will be seen, although the two types of fibre differ in detail in their luminescence response, the variations are small and are unlikely to be attributable to impurity doping at the 1% level. The fibre substrates are drawn using standard Heraelux WG, from Hereaus Silica and Metals Ltd tubing. Only in two cases (ND324 and ND297) was Cl_2 gas used in the drying stage after doping. Finally a sample N9 was prepared without a core but processed into fibres. This was done to compare effects of draw-

Table 1. Details of the impurities added into the core and cladding regions of the fibres. Note that the pulling speeds and melt temperatures have also been varied.

Fibre number	Wt% GeO_2 in core	Core dopant		Pulling temperature (°C)	Pulling speed (rpm) or m min^{-1}	
ND297-04	19	Nd; 1400 ppm		2150	550	31
ND324-01	11	Ho; 200 ppm		2097	400	22.6
ND325-01	10	Nd; 225 ppm		2065	380	21.6
ND414-01	6	Er; 1100 ppm Yb; 4500 ppm		2100	300	17
Substrate N9	—	—		2108	480	27
Preform number		Core	Cladding	—	—	
ND414	6	Er,Yb	~ 1% P ~ 1% F	—	—	
ND416	6	Nd	—	—	—	
ND424	6	—	—	—	—	

ing speed and melt temperatures on defects which are quenched into the substrate.

The experimental arrangements for recording luminescence spectra during x-ray irradiation, electron beam bombardment or thermoluminescence were similar, although different sets of equipment were used for the cathodoluminescence (CL) and the radioluminescence (RL) and thermoluminescence (TL). The basic lay-out of the components is sketched in figure 1. The radio and cathodoluminescence systems each include an $f/4$ scanning monochromator, pulse counting or phase sensitive detection (for CL) using a cooled red sensitive photomultiplier (S20 photocathode). A small microcomputer system records the temperature, intensity and wavelength data. In all cases the spectra were corrected for the wavelength-dependent efficiency of the system. This is an essential step, as over the spectral range investigated the combination of photomultiplier response and diffraction grating efficiency causes the overall sensitivity to vary by more than a factor of 100.

Radioluminescence (RL) spectra were taken during excitation with 30 kVp x-rays with a tube current of 15 mA which delivers some 30 Gy min^{-1} at the sample. Fresh samples were normally used for each set of measurements as the emission spectra may change after irradiation and heating cycles. Cathodoluminescence (CL) was excited with 10 keV electrons at a 1 μA beam current. Because of the limited penetration of the electron beam, only preforms of fibres, or bulk silica, were recorded. Signals were obtained separately from the substrate tube and from the central core region. One further advantage of the CL system is that one can modulate the electron beam and then use phase sensitive detection to aid resolution of luminescence bands of different excited state lifetimes.

The major problem with the luminescence studies of the fibres is that the samples are not strongly luminescent and hence there is a problem of signal to noise. This is most apparent in the red end of the spectra because of the poor efficiency of both the photomultiplier tubes and the gratings in the red region. In principle one might improve the signal-to-noise ratio (SNR) by increasing the exposure time and better signal averaging, but this approach must be used with caution as invariably the spectra and relative intensities of the emission bands change with accumulated irradiation dose.

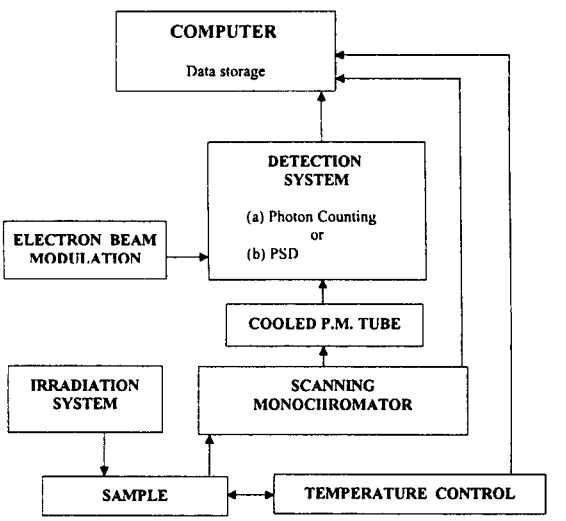

Figure 1. A schema of the experimental luminescence system. The scanning monochromator has $f/4$ optics and detection is by a cooled PM tube with data recording by a computer. The sample temperature is controllable from 40 K to 400 °C. The radiation sources are either an x-ray set or an electron beam. For the electron beam, modulation is used in conjunction with a PSD.

Temperature control was available either by a cryostat from 40 to 300 K or by a heater above room temperature from 20 to 400 °C.

3. Results and comments

3.1. Examples of radioluminescence spectra

Before proceeding to data for the optical fibres it is worth viewing the RL signals obtained from the simpler pure silica material. This is shown in figure 2 as an isometric plot of signal against wavelength and temperature. In the case of silica there is a strong signal, hence the wealth of emission bands and temperature variations

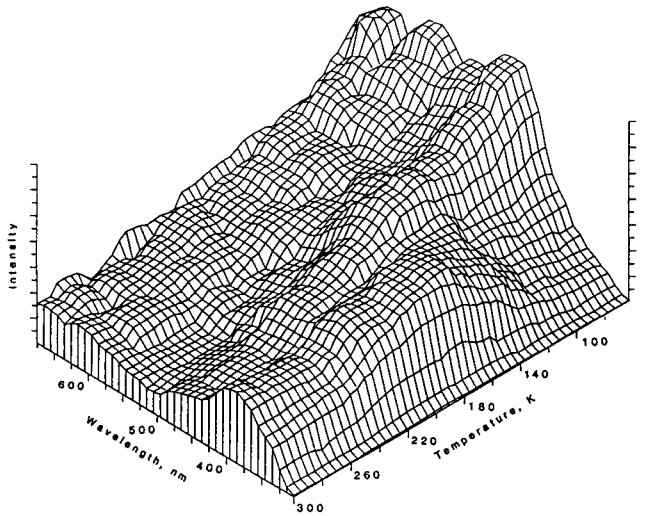

Figure 2. An isometric plot of the radioluminescence intensity against wavelength and temperature for a sample of Spectrosil silica.

recorded here represent actual changes. Unfortunately, for the fibre examples, there will be greater uncertainty as to which of the minor variations are sample effects and which are merely the result of experimental difficulty. For silica there is an obvious difference between the temperature behaviour of the band near 400 nm and the signals from 450 to 700 nm, with the general increase in the red end of the spectra at low temperature, whereas the blue signal passes through a maximum intensity near 180 K. Emission features peak near 460, 520, 580 and 640 nm at 70 K.

Isometric plots of the temperature variations of the RL spectra for fibres and preforms are given in figure 3. Figure 3(*a*) is for the preform ND414, figure 3(*b*) is for the preform ND416 and figure 3(*c*) is for the fibre drawn from ND414. It is immediately obvious that compared with the silica example, the emission is predominantly at shorter wavelengths and there are negligible detectable signals beyond about 600 nm. Closer inspection of figure 3 reveals significant differences between the relative intensities of the component features. This is most obvious for the two preforms. Additionally, minor differences are apparent for the fibre and preform version of ND414. The data of figure 3 are broadly representative of many of the germanosilicate optical fibres studied.

In studies of the dose dependence of the RL signals for a piece of bulk silica and preforms numbers ND414, ND416 and ND424 the samples ND414 and ND416 are quite similar but the purer examples of ND424 (for which there is no Ge additive in the core) and bulk silica have a pronounced red signal in addition to the blue emission. In all cases the intensity is not constant but the component emission bands grow at different rates. This is most apparent for the silica where the 400 nm band grows rapidly relative to the 460 nm band. Although not clearly resolved, the broad blue envelope of all samples contains evidence for peaks variously near 350, 380, 400 and 460 nm.

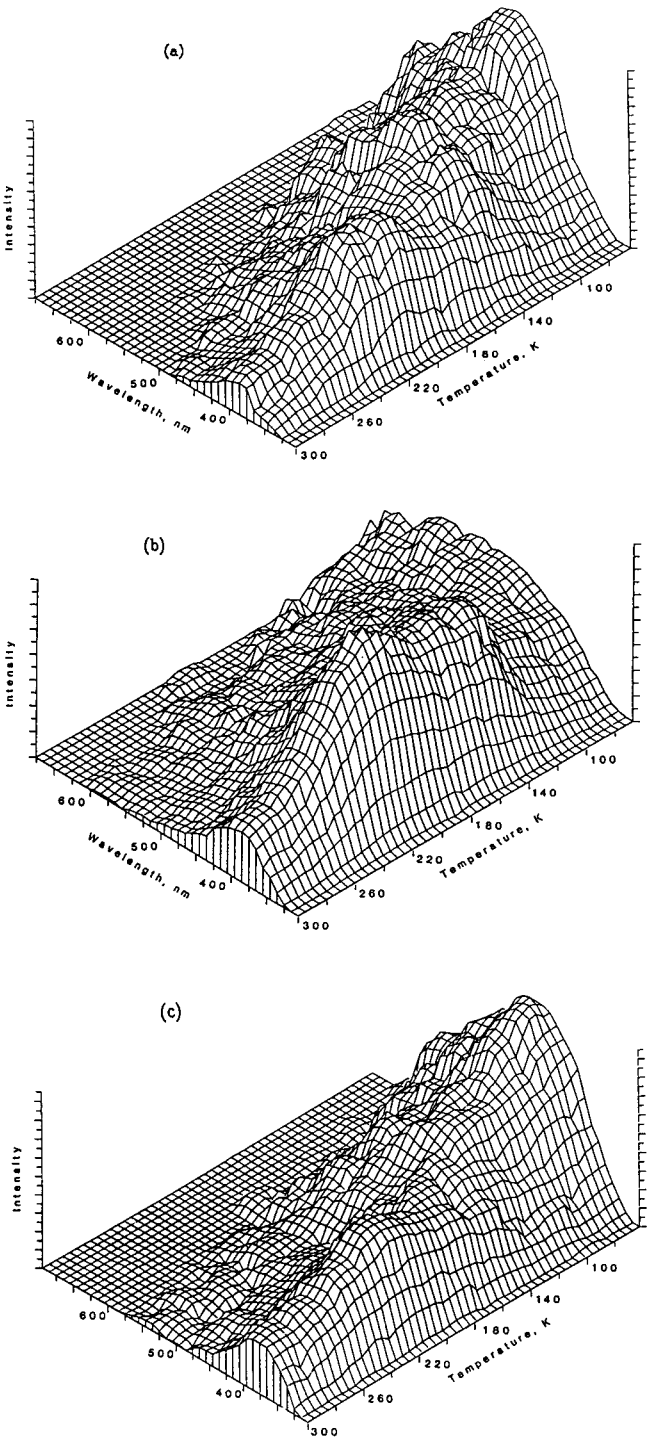

Figure 3. Isometric RL data for two fibre preforms (*a*) ND414, (*b*) ND416 compared with the RL signal from a fibre of the type ND414.

3.2. Luminescence sensitivity

Whilst the data show considerable similarity in the emission spectra they disguise the fact that the relative luminescence intensities differ significantly between these examples. The sample ND414 is much brighter than ND416 despite the similarity in spectra. ND414 is also brighter than ND324. It is significant, however, that ND414 is more heavily doped than either ND416 or ND324 (table 1). At first sight the variations in luminescence efficiency are surprising as the substrate material

Table 2. Some frequently reported luminescence bands found in quartz and silica. Indications of possible defect models are given.

Band (RT)			
nm	eV	Method†	Possible models for origin
260	4.77	CL	Oxygen vacancy
290	4.28	PL,CL	Oxygen vacancy
380	3.25	RL,CL	Aluminium impurity, an impurity imported during growth of quartz
390	3.17	RL	E'_β
400	3.1	PL	O_2 intrinsic defects and Ge impurity
450–480	2.5–2.8	RL,CL	Recombination of self-trapped exciton
580	2.15	CL	Oxygen vacancy
640	1.9	IBI,CL	Oxygen vacancy and Na impurity

† CL, PL, RL are cathodo-, photo- and radioluminescence and IBI is ion beam implantation.

is common throughout and the doped core represents perhaps only 5% of the total fibre cross section. Nevertheless, the addition of impurity dopants and/or intrinsic defects in the core has changed the overall efficiency of light production, even though the same basic recombination centres appear to exist in most of the fibres (except that the purer materials have stronger red emission bands). Intrinsic defect features can be influenced by rapidly cooling material from the melt, as during fibre drawing. Such processing amplified the emission intensity of the ND414 preform to fibre example. A combination of impurity and quenched-in defects may thus be assumed to give a brighter signal from ND297 and ND324 since (see table 1) ND297 has some seven times as many rare earth dopants in the core and was pulled both from a higher temperature and at a faster rate than ND324. Indeed, the observation is that ND297 is relatively bright compared with ND324.

4. Cathodoluminescence

As for the RL data it is initially useful to note the emission spectra from pure silica. The cathodoluminescence spectrum taken at room temperature is shown in figure 4(*a*) for a silica sample. Using a modulation frequency of 90 Hz there are well resolved bands at 360, 470 and 670 nm with evidence for a weaker signal near 580 nm. The fibre preform signals are similar—for example figures 4(*b*), 4(*c*) and 5(*a*) show preforms of ND416, ND297 and ND414—but they lack a clearly resolved feature at 360 nm emission, although the other components are normally apparent. In the fibre preform material the intensity rises on cooling from 300 to 40 K, by a factor of ten for the red peak and four for the blue. Further, the blue maximum shifts from 460 to 480 nm (figure 5(*b*)). Note, however, that in making such comparisons it is essential to specify the modulation frequency since, as has been noted in other silica and silicate glass studies, the lifetimes of the blue and red emission bands differ, and hence changes in modulation frequency alter the shape of the spectra. No detailed attempt has been made here to resolve all the component bands fully but, on altering the modulation frequency from 90 to 9 Hz, the 400 nm signal is enhanced relative to the 460 and 670 nm signals, as shown by comparing figures 5(*a*) and 5(*c*). Changes at such low modulation frequencies imply that the 400 nm excited state has a lifetime of some tens of milliseconds. Whilst direct current measurements are least likely to distort the spectra if there is a variety of lifetime components, in practice this is experimentally awkward for CL as light from the DC electron gun filament is strongly reflected into the monochromator and so beam modulation and phase sensitive detection are used to reject this scattered light. Note that in this experiment the light scattered from the filament is comparable in intensity to that from the CL of the fibres and preforms.

Both RL and CL show a mixture of emission bands near 400 and 460 nm but their relative intensities are different and depend strongly on modulation frequency. In CL recorded at 90 Hz, and with a much higher ionization density than for RL, the 460 nm signal is greater than that at 400 nm. Note that this is consistent with the similar situation of intense local ionization generated by ion beam excitation in which the apparent peak of the luminescence envelope is invariably near 460 nm.

One of the advantages of CL is that the electron beam can be localized into a small region and hence it should be possible to emphasize differences between the core and substrate regions. In this work a copper aperture with a one millimetre diameter was used to select various regions. For the fibre preforms with a millimetre size core this meant that core features could be selectively excited and contrasted with signals from substrate regions. The aperture method is adequate for the substrate but is not 100% specific for the central area, which includes the core plus cladding and traces of the substrate. Such a separation of regions was not possible with RL. Signals recorded at 90 Hz are presented in figures 5(*d*) and 5(*a*) for the core and substrate of ND414. It is strikingly evident that the core signal is primarily at 400 nm.

There are also obvious similarities with the RL data in that for the relatively pure substrate there is a strong red emission (670 nm), a peak near 460 nm and shoulders or minor peaks at 400 and 580 nm. By contrast, the predominantly core region has only weak signals in the red end of the spectrum. From the asymmetry of the

peak one can assume that there is still a 460 nm component, and this can further be confirmed by comparing rather similar materials such as those from ND414 and ND416.

5. Discussion

The blue luminescence excited by ionization of germanosilicate optical fibres and preforms resembles that generated in silica glass and crystalline quartz. This is not unexpected since all the examples are similar on the scale of local defects based on the silicate tetrahedron structure. Luminescence generated by relaxation of self-trapped excitons, or recombination at the oxygen defects such as the E′-type centres will only be marginally influenced by differences in the long-range structure. The isometric and dose-dependent signals displayed above confirm that many of the same emission bands are involved in all cases, although both their relative intensities and their absolute luminescence efficiency may differ.

As cited in section 1, the 'intrinsic' electron–hole recombination from an STE has been suggested to be near 440 to 460 nm. Modifications of the local site symmetry from impurities, stresses and broken bonds modify the exact wavelength of the emission. A signal near 460 nm is seen in all cases and this must be assumed to arise both from the large volume of the substrate and from the smaller core and cladding region of the fibres. Fortunately, for the present study, the fabrication methods used to make optical waveguides inevitably generate higher dopant and defect concentrations within the core and cladding. Consequently the luminescence efficiency is greatly enhanced in these regions and so the overall luminescence response is quite sensitive to the fabrication process. Several general trends can be seen from the data. It is expected that in a pure silica sample the STE relaxation will always be apparent near 460 nm. However, if the overall efficiency of this intrinsic decay path is small and the excitons are mobile in the pure silica, then the intrinsic features will be suppressed if there are high concentrations of imperfect lattice sites which can provide efficient exciton recombination centres. This was clearly demonstrated for the comparison of core and substrate data with CL.

One should note that there are significant differences between RL and CL (and also ion beam excited luminescence). One obvious difference between the methods of excitation is that for the x-ray irradiation the ionization density is much lower than for either the CL or ion beam case and, furthermore, the efficiency of producing new defects increases with ionization density. The defects may be only metastable, but for a dynamic luminescence experiment their lifetimes may significantly influence the emission spectra. Hence, one possible explanation of the spectral differences is that exciton capture is favoured at impurity sites if the impurity concentration is high relative to the exciton density.

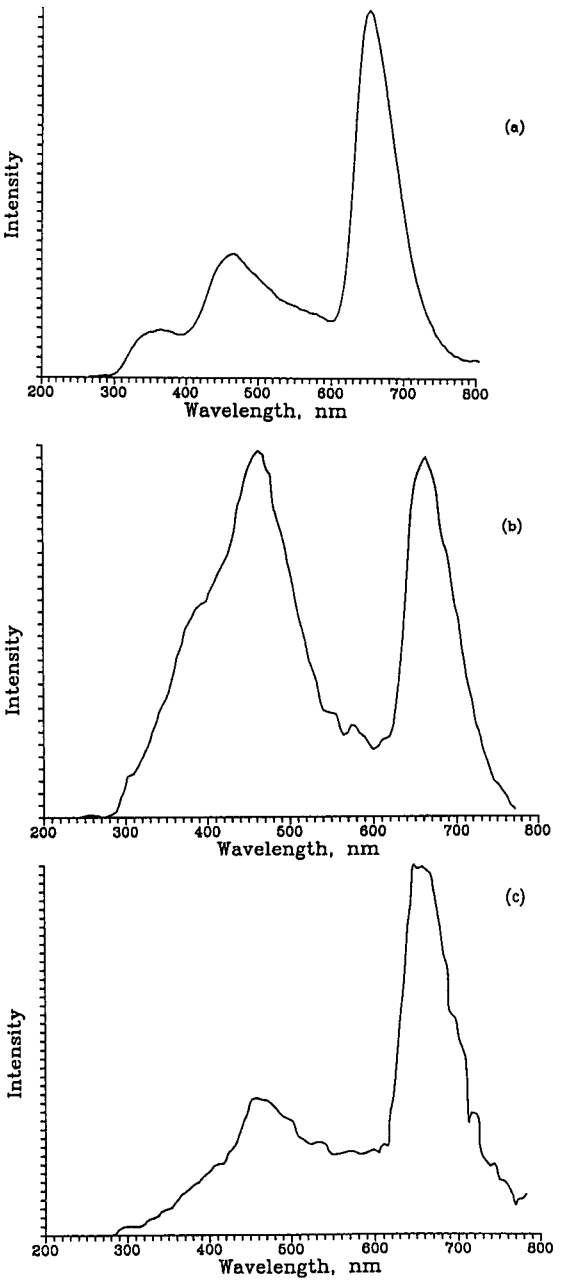

Figure 4. A cathodoluminescence spectrum obtained at room temperature taken with a modulation frequency of 90 Hz. (*a*) A silica sample, (*b*) CL signals from the fibre preform ND416, and (*c*) fibre type ND297.

So for low ionization densities the imperfections provide a significant set of decay paths, whereas at high ionization intensities (i.e. in CL) there are insufficient impurities relative to the exciton production rates, and hence the competitive decay routes will be biased toward the intrinsic luminescence. The overall conclusion is that the 460 nm emission is purely intrinsic exciton decay.

A further observation is that the purer and more perfect materials emit more strongly in the red end of the spectrum. Slightly less obvious is that the purer samples show more clearly resolved features in the envelope of bands at the blue region. Defects formed during ion bombardment of pure silica suppress the red emission. Although the signals at 640 to 670 nm have been sug-

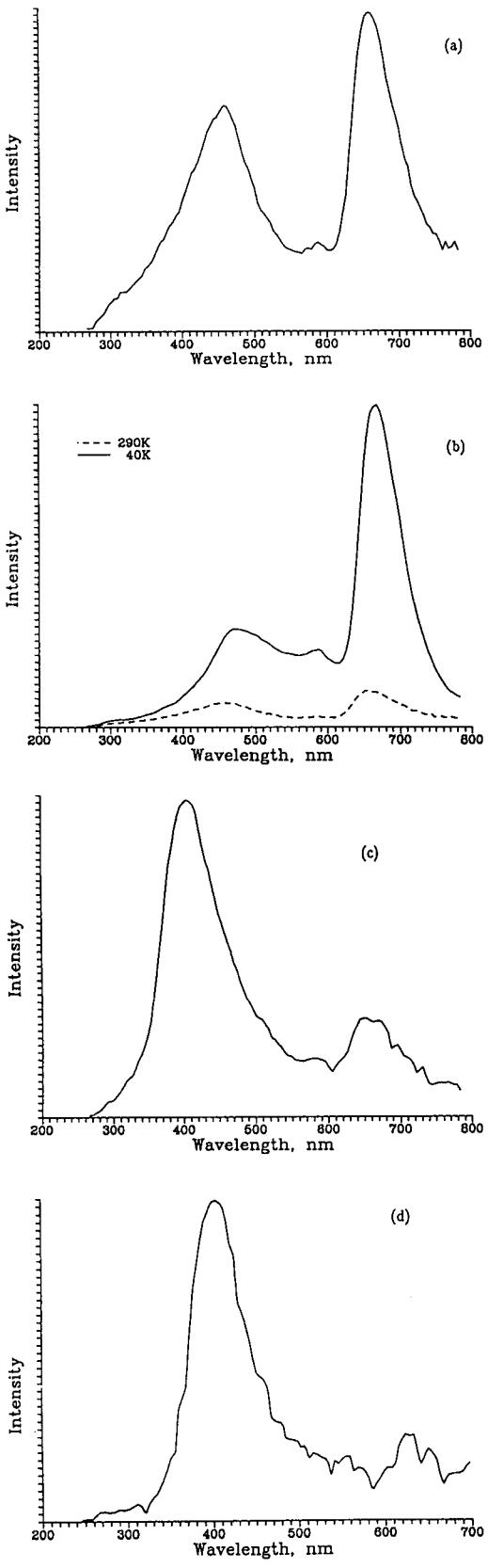

Figure 5. Examples of CL from fibre type ND414. (*a*) At room temperature and 90 Hz, (*b*) data at 290 and 40 K, (*c*) at 9 Hz and (*d*) at 90 Hz with the beam centred on the fibre core.

gested by various authors to be linked to alkali impurity ions, one cannot exclude a decay route of an exciton at a distorted silicate site. Fibre growth defects apparently do not totally remove this decay route as red emission is seen in CL of fibres and preforms.

The common impurity, which is deliberately added into many of the fibre cores, is germanium. It is therefore tempting to ascribe the strong core luminescence at 400 nm to a germanium impurity defect, as claimed by several authors (Turner and Lee 1965, Skuja and Trukhin 1989). Data, such as those presented in figures 4 and 5, are totally consistent with this model for Ge recombination sites producing the 400 nm emission, and further, the CL results suggest that the process involves a very long excited state lifetime. There is supportive evidence for assignment of this luminescence to Ge from the TL work in quartz in which it is proposed (Yang and McKeever 1990a, b) that an oxygen vacancy linked to Ge emits at 400 nm whereas H_3O_4 and AlO_4 sites provide 380 and 470 nm light respectively.

Whilst the present results strongly support a model in which luminescence at a germanium impurity site generates 400 nm emission, it is far less clear what is the detailed structure of the site. As reviewed by Russell *et al* (1990), the Ge ions may not only be in the form of isolated defects but may exist in a variety of Ge E′-type centres analogous to the normal Si E′-type defects. Additionally, there are theoretical suggestions (Cormack 1991) that impurity ions in the glass may associate in pairs or chains of impurities. In such a non-random distribution of the Ge impurities one would find adjacent GeO_4 tetrahedra linked together. Consequently, irradiation could locally destroy such Ge pair bonding and this would increase the effectiveness of the isolated Ge luminescence sites. Hence the 400 nm signal might be assumed to increase with irradiation dose, as was experimentally observed.

It is also interesting to speculate on the relevance of these new luminescence data to the photorefractive changes induced in a Ge-doped fibre, as reviewed by Russell *et al* (1990). For the photorefractive change a key step in the process is the relaxation of the local bond structure to alter the refractive index. It is suggested that the dissociation of defect complexes which involve linked GeO_4 groups may be relevant. This is a reversible change—however, it is not a one-step process but instead is thought to involve a two-photon absorption. At the power levels at which the photorefractive effect is seen, a conventional two-photon absorption event may be a little unexpected. However, reference to the current CL data emphasizes that excited Ge recombination sites develop which are long lived, on the scale of tens of milliseconds. Such a situation is favourable for excited state absorption and hence an overall two-photon absorption process may be more feasible than one would at first suspect.

When discussing the other luminescence bands and their associated defect sites the examples of RL from preform and fibre suggest that, although the concentrations of defects differ (i.e. more in the fibre), the defect types are very similar. It is also evident that if the defects are often perturbations of a simple broken oxygen bond site then the emission bands can overlap, so several

defect types can produce similar wavelengths. Resolution of component luminescence sites can be achieved by observing the temperature dependence of the signal, noting the dose dependence or combining a radiation and heating cycle to the measurements. For example, in the present study, the bands near 380–390 nm show an unusual temperature dependence, with growth in intensity peaking between 150 and 220 K. This behaviour is paralleled by the response of the E'_β centre identified in 'wet' silica by Griscom (1985) and Tsai *et al* (1987) using electron paramagnetic resonance. Whilst considerable care has been taken to exclude OH ions from the optical fibre cores it should be recalled that luminescence is capable of detecting defect concentrations of less than 1 in 10^9, and hence an association with traces of OH may be of value in monitoring the fabrication procedure.

Models for the defect sites of other silica emission bands include assignment of a 580 nm signal to e–h recombination between oxygen vacancies and O_2 linkages. The presence of a band near 580 to 590 nm in the current study is in broad agreement with this intrinsic type model. The 640 nm band in silica has been seen by several authors and variously ascribed to impurity (possibly sodium) ions near an E′ complex. In several cases the intensity of the red emission has decreased with damage. The suggestion of an intrinsic defect site which becomes non-radiative by association with other defects or impurities has some support from the present work in that the band is not clearly resolved in all the samples and so is unlikely to be a 'pure' intrinsic defect. It is also expected that the dopants added to the fibre cores, and the presence of defects quenched into the material during fibre drawing should lead to many complex defect sites and hence suppression of a sensitive feature such as the 640 nm signal. For example, Friebele (1979) has reported that the presence of P ions decreases luminescence intensity.

Table 2 summarizes the preceding discussion of bands and possible models. Many emission bands derive from a complex amalgam of intrinsic and E′-type defects, coupled with site-specific impurity emission. One may make tentative assignments to the defect structures using the literature for quartz and silica luminescence. However, the crystalline and amorphous variants differ in that ionization can generate new stable defects in silica whereas only transient unstable defects form in the ordered structure. This is in agreement with the silica and fibre data in which prolonged irradiation alters the luminescence intensity. Damage production of E′-type defects is also consistent with the presence of several emission bands which extend throughout the low-temperature range.

6. Conclusion

The luminescence signals from optical fibres provide a highly complex but sensitive probe of the defects in the cores of the fibres, despite the presence of signal from the much larger volume of substrate. Consequently the luminescence offers a method of following changes in fabrication procedure. If one can further correlate the luminescence with the optical properties of the fibres then it could become a routine control technique.

At the more fundamental level of understanding the interactions of point defects in the fibre glasses the luminescence data so far show a wide variety of defect sites but these can broadly be interpreted in terms of familiar properties of excitons and oxygen vacancy defect sites in the silicate groups. In particular, the present study confirms the role of Ge impurities as the source of the 400 nm emission from the core and exciton decay as generating the signals near 460 nm.

Acknowledgments

We are grateful to the Iranian Ministry of Culture and Higher Education and the Optical Research Centre in Southampton for financial support.

References

Abu Hassan L H, Townsend P D and Wood R A 1988 *Nucl. Instrum. Methods* B **32** 295–30
Alonso P J, Halliburton L E, Kohnke E E and Bossoli R B 1983 *J. Appl. Phys.* **54** 5369–75
Cormack A N 1991 private communication
Ellis, A E, Moskowitz P D, Townsend J E and Townsend P D 1989 *J. Phys. D: Appl. Phys.* **22** 1758–62
Friebele E J 1979 *Opt. Eng.* **18** 552–61
Grinfelds A U, Aboltyn D E and Plekhanov V G 1984 *Sov. Phys. Solid State* **26** 1075–77
Griscom D L 1985 *J. Non-Cryst. Solids* **73** 51–7
Itoh C, Suzuki T and Itoh N 1990 *Phys. Rev.* B **41** 3794–9
Itoh C, Tanimura K and Itoh N 1988 *J. Phys.* C **21** 4693–702
—— 1989 *Phys. Rev.* B **39** 11183–6
Jaque F and Townsend P D 1981 *Nucl. Instrum. Methods* **182/183** 781–6
Malik D M, Kohnke E E and Sibley W A 1981 *J. Appl. Phys.* **52** 3600–5
Mattern P L, Lengweiler K and Levy P W 1975 *Radiat. Effects* **26** 237–48
McKeever S W S 1984 *Radiat. Prot. Dosim.* **8** 81–98
—— 1985 *Thermoluminescence of Solids* (Cambridge: Cambridge University Press)
Nagel S R, MacChesney J B and Walker K L 1982 *IEEE J. Quant. Electron.* **15** 459–76
Russell P St J, Poyntz-Wright L J and Hand D P 1990 *SPIE Fiber Laser Sources Amp.* **1373** 126–39
Skuja S N and Trukhin A N 1989 *Phys. Rev.* B **39** 3990–11
Tanimura K and Halliburton L E 1986 *Phys. Rev.* B **34** 2933–5
Townsend J E, Poole S B and Payne D N 1987 *Electron. Lett.* **23** 329–31
Trukhin A N and Plaudis A E 1979 *Sov. Phys. Solid State* **21** 644–6
Tsai T E, Griscom D L and Friebele E J 1987 *Diff. Def. Data* **53/54** 469–76
Turner W H and Lee H A 1965 *J. Chem. Phys.* **43** 1428–9
Wang P W, Albridge R G, Kinser D L, Weeks R A and Tolk N H 1991 *Nucl. Instrum. Methods* **B59/60** 1317–19
Yang X H and McKeever S W S 1988 *Nucl. Tracks Radiat. Meas.* **14** 75–9
—— 1990a *J. Phys. D: Appl. Phys.* **23** 237–44
—— 1990b *Radiat. Prot. Dosim.* **33** 27–30